J|A|C|S COMMUNICATIONS

Published on Web 07/01/2009

Is There a Ni-Methyl Intermediate in the Mechanism of Methyl-Coenzyme M Reductase?

Shi-lu Chen,*,† Vladimir Pelmenschikov,‡ Margareta R. A. Blomberg,† and Per E. M. Siegbahn*,†

Department of Physics, Stockholm University, SE-10691 Stockholm, Sweden, and Scientific Computing and Modelling NV, Theoretical Chemistry, Vrije Universiteit, De Boelelaan 1083, NL-1081 HV Amsterdam, The Netherlands

Received May 27, 2009; E-mail: shlchen@physto.se; ps@physto.se

Methyl-coenzyme M reductase (MCR) is a nickel-containing enzyme responsible for the last step of methanogenesis in methanogenic archaeabacteria.[1] It catalyzes the conversion of methyl-coenzyme M (CH_3-SCoM) and coenzyme B ($CoB-SH$) to methane and the heterodisulfide ($CoM-S-S-CoB$), using a nickel(I) porphyrinoid cofactor, $Ni(I)F_{430}$.[1] Two main catalytic mechanisms have been proposed. Mechanism I proceeds via an organometallic methyl$-Ni(III)F_{430}$ intermediate (referred to as MCR_{Me}),[2] while mechanism II includes a methyl radical and a $CoM-S-Ni(II)F_{430}$ intermediate.[3] Although the crucial MCR_{Me} has been characterized from the active MCR (MCR_{red1}) and methyl bromide[4] or iodide,[5] its formation from the native substrate (CH_3-SCoM) has never been found. Thus, scrutiny into the formation of the $CH_3-Ni(F_{430})$ species in MCR is of significance for the interpretation of the MCR reaction mechanisms.

In the present work, using density functional theory (DFT) with the hybrid functional B3LYP as implemented in Jaguar 7.0 and Gaussian 03 packages,[6] we have investigated the formation of the methyl$-Ni(F_{430})$ species in MCR with CH_3-I, CH_3-Br, CH_3-Cl, and CH_3-S-CH_3 as substrates. Herein, the CH_3-S-CH_3 is regarded as a model of the native substrate (CH_3-SCoM), while methyl halides can also be considered to represent various halogenated sulfonates and carboxylates, which are frequently employed as inhibitors for the MCR_{red1}.[7−9] We here present the energetics for the formation of the methyl$-Ni(F_{430})$ species and provide the characterization of the transition states and intermediates involved.

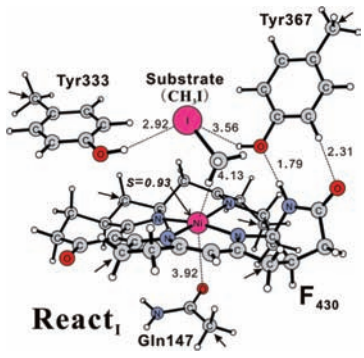

Figure 1. Optimized structure of the MCR active site with CH_3-I bound. Arrows indicate atoms that are fixed to their X-ray positions. All distances are given in angstrom (Å). The unpaired spin population is shown also.

We used the high resolution crystal structure (PDB code 1HBN)[10] to construct a model of the active site of MCR (Figure 1). The model contains the $Ni(F_{430})$ cofactor, two tyrosines (Tyr333 and Tyr367), and the Gln147. To reduce the size, some truncations have been made. The methyl, acetamide, and carboxylate substituents in F_{430} were replaced by hydrogens. The Gln147 and tyrosines were represented by acetamide and *p*-methyl phenols, respectively. The total charge of the model is zero, and the total number of atoms without substrates included is 102. To avoid unorderly movement, the atoms where the truncations were done were fixed to their X-ray crystal positions. With substrates included, the overall geometric parameters obtained from the geometry optimization of the present model of the MCR active site agree well with the experiments and previous calculations. For example, with CH_3-I as the substrate (Figure 1), the distances of Ni to the four ligated nitrogens of F_{430} are calculated to be 2.02, 2.07, 2.02, and 2.17 Å, to be compared to the crystallographic values 2.04, 2.10, 2.07, and 2.10 Å,[10] the PW91-computed distances 1.98, 2.03, 2.00, and 2.14 Å,[11] and the EXAFS-fitted distances 2.05 Å.[12] The substrate is loosely bound at the active site. The optimized enzyme−substrate complex, $\mathbf{React_I}$, is shown to be in the †Ni(I) state with an unpaired spin of 0.93 and a charge of 0.20 at the Ni atom (see entry 1 in Table 1).

Table 1. Properties of Stationary Points in the $CH_3-Ni(F_{430})$ Formation

entry	complex[a]	spin/charge: Ni	spin/charge: I, Br, Cl, or S	spin/charge: C_m[b]	energy (kcal/mol)
1	$React_I$	0.93/0.20	0.00/0.03	0.00/−0.71	0.0
2	$TS1_I$	1.03/0.22	−0.09/−0.25	−0.10/−0.58	3.9
3	$Int1_I$	1.28/0.26	−0.20/−0.48	−0.32/−0.45	−5.3
4	$TS2_I$	1.27/0.24	−0.15/−0.48	−0.35/−0.42	−2.6
5	$Int2_I$	1.31/0.22	−0.17/−0.52	−0.39/−0.42	−3.8
6	$TS3_I$	1.16/0.26	−0.14/−0.34	−0.21/−0.52	9.5
7	$React_{Br}$	0.93/0.20	0.00/−0.08	0.00/−0.62	0.0
8	$TS1_{Br}$	0.97/0.20	−0.05/−0.25	−0.07/−0.53	4.9
9	$Int1_{Br}$	1.25/0.32	−0.17/−0.53	−0.32/−0.42	−3.3
10	$TS2_{Br}$	1.25/0.29	−0.13/−0.54	−0.36/−0.39	−1.7
11	$Int2_{Br}$	1.29/0.27	−0.15/−0.56	−0.40/−0.39	−2.5
12	$TS3_{Br}$	0.96/0.19	−0.03/−0.19	−0.04/−0.56	11.0
13	$React_{Cl}$	0.93/0.20	0.00/−0.12	0.00/−0.57	0.0
14	$TS1_{Cl}$	0.98/0.19	−0.04/−0.31	−0.09/−0.49	6.6
15	$Int1_{Cl}$	1.23/0.31	−0.12/−0.54	−0.34/−0.40	−0.7
16	$TS2_{Cl}$	1.23/0.29	−0.09/−0.57	−0.37/−0.37	0.5
17	$Int2_{Cl}$	1.27/0.27	−0.11/−0.58	−0.42/−0.37	−0.3
18	$TS3_{Cl}$	0.97/0.18	−0.03/−0.26	−0.06/−0.51	13.0
19	$React_S$	0.93/0.22	0.00/0.13	0.00/−0.64	0.0
20	TS_S	1.15/0.23	−0.18/−0.20	−0.15/−0.45	27.0
21	Int_S	1.29/0.27	−0.28/−0.28	−0.24/−0.43	26.6

[a] Abbreviations signify reacting state (React), TS for methyl transfer (TS1), pentacoordinated $CH_3-Ni(F_{430})$ intermediate (Int1), TS for Gln147 oxygen binding (TS2), hexacoordinated $CH_3-Ni(F_{430})$ intermediate (Int2), and the concerted TS (TS3); subscripts indicate the CH_3-I (I), CH_3-Br (Br), CH_3-Cl (Cl), and CH_3-S-CH_3 (S) substrates. [b] Carbon of the transferred methyl.

From $\mathbf{React_I}$, a transition state (TS) for the methyl transfer from the CH_3-I substrate to the Ni ($\mathbf{TS1_I}$, Figure 2) has been optimized and confirmed to be a first-order saddle point with an imaginary frequency of 216*i* cm^{-1}. At $\mathbf{TS1_I}$, the key distances of the methyl carbon (C_m) to the iodine and Ni are 2.49 and 2.55 Å, respectively. With solvation effects of the surrounding protein included (calcu-

† Stockholm University.
‡ Vrije Universiteit.

10.1021/ja904301f CCC: $40.75

lated with the self-consistent reaction field method, using a Poisson−Boltzmann solver[13]), the calculated barrier for this step is very low with 3.9 kcal/mol (Table 1, entry 2).

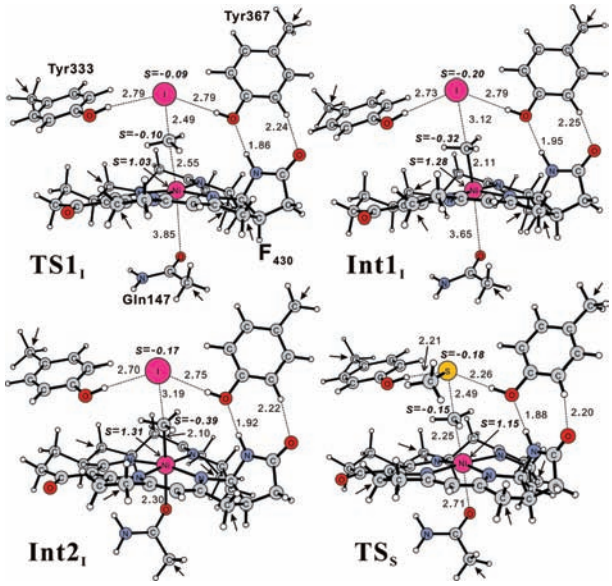

Figure 2. Optimized structures of the transition state for methyl transfer (**$TS1_I$**) and the resulting penta- (**$Int1_I$**) and hexacoordinated (**$Int2_I$**) $CH_3-Ni(F_{430})$ intermediates in the CH_3-I reaction and of the transition state for the formation of $CH_3-Ni(F_{430})$ in the CH_3-S-CH_3 reaction (**TS_S**).

The methyl transfer leads to a pentacoordinated $CH_3-Ni(F_{430})$ intermediate (**$Int1_I$**, Figure 2), which is found to lie 5.3 kcal/mol lower than **$React_I$**. The increased spin densities at the Ni (1.28) and C_m (−0.32) atoms point out that this $CH_3-Ni(F_{430})$ species is in a resonance state between the $^{1}CH_3-{}^{II}Ni(II)$ radical state and $CH_3^{-}-{}^{I}Ni(III)F_{430}$.[4,5] This state is consistent with the assignment of the alkyl−$Ni(F_{430})$ state (MCR_{BPS}) formed from the MCR_{red1} and 3-bromopropanesulfonate (BPS).[7] The resulting iodine ion (I^-) is contaminated by the Ni−methyl radical to have a spin of −0.20. The two tyrosines stabilize the leaving I^-, facilitating the cleavage of the $I-C_m$ bond, a role that is of importance especially when considering that the MCR active-site pocket is hydrophobic and the docked substrate has to be stripped of water.[10] In **$Int1_I$**, the $Ni-C_m$ bond distance is computed to be 2.11 Å, which is reasonably well in line with an average distance of ∼2.04 Å based on EXAFS data analysis and TD-DFT calculations.[12]

From **$Int1_I$**, overcoming a very small barrier of 2.7 kcal/mol, the Gln147 oxygen coordinates to Ni, leading to a hexacoordinated $CH_3-Ni(F_{430})$ species (**$Int2_I$**, Figure 2). The TS for Gln147 binding (**$TS2_I$**) is given in the Supporting Information (SI). This binding slightly increases the energy of the complex by 1.5 kcal/mol but hardly changes any electronic properties (Table 1, entries 3 and 5). Therefore, it is probably difficult to distinguish the penta- from the hexacoordinated $CH_3-Ni(F_{430})$ intermediates experimentally.

A concerted TS connecting **$React_I$** with **$Int2_I$** (**$TS3_I$**, in SI) has also been obtained. Via **$TS3_I$**, it turns out that, simultaneously with the binding of the Gln147 oxygen to Ni, the methyl is transferred from the substrate to Ni, directly resulting in the hexacoordinated $CH_3-Ni(F_{430})$ intermediate (**$Int2_I$**). However, the barrier for this concerted process is predicted to be much higher (9.5 kcal/mol) than that of the stepwise process presented above (3.9 kcal/mol), indicating that the individual methyl transfer followed by the binding of the Gln147 oxygen is the preferred pathway for formation of the hexacoordinated $CH_3-Ni(F_{430})$ intermediate.

The reactions of the CH_3-Br and CH_3-Cl substrates follow the same pattern as the case of CH_3-I, and similar stationary points have been optimized (see SI for geometries and Table 1 for properties). The corresponding reaction barriers are calculated to be feasible, 4.9 and 6.6 kcal/mol for CH_3-Br and CH_3-Cl, respectively (Table 1, entries 8 and 14). It can thus be concluded that the reactions of MCR_{red1} with alkyl halides are accessible, as observed experimentally.[4,5,7−9]

When CH_3-S-CH_3 was chosen as the substrate, only the concerted TS (**TS_S**, Figure 2) and hexacoordinated $CH_3-Ni(F_{430})$ intermediate (**Int_S**, given in SI) could be located. Without the stabilization provided by the Gln147,[3] no $CH_3-Ni(F_{430})$ species can be optimized in this case. In contrast to the exothermicity of the reactions of methyl halides, the reaction of CH_3-S-CH_3 is calculated to be strongly endothermic by 26.6 kcal/mol, with a barrier of 27.0 kcal/mol (Table 1). Consistent with the energetics, the optimized **TS_S** is very late (Figure 2). To consider the effect of CoB−SH (cosubstrate), we added a CH_3-SH to the complexes and reoptimized the reactant, TS, and $CH_3-Ni(F_{430})$ intermediate for the CH_3-S-CH_3 reaction (see SI for geometries). The updated endothermicity and barrier are 23.5 and 24.0 kcal/mol, respectively. This clearly demonstrates that the formation of the $CH_3-Ni(F_{430})$ species from the MCR_{red1} and native substrate (CH_3-SCoM) is unreachable. In contrast, the reverse reaction of $CH_3-Ni(F_{430})$ with coenzyme M (H−SCoM) or thiols, leading to the regenerated MCR_{red1}, should be favorable, as shown by experiments.[5,9]

In summary, our calculations indicate that the formation of the methyl−$Ni(F_{430})$ species in MCR is dependent on the acidity of the substrate leaving group. In particular, it has been demonstrated that the main flaw in mechanism I is the impossibility of the methyl−$Ni(F_{430})$ formation. This step is predicted to be endothermic by 23.5 kcal/mol.

Acknowledgment. This work has been supported by the Carl Trygger Foundation.

Supporting Information Available: Computational details and Cartesian coordinates and absolute energies of all optimized structures. This material is available free of charge via the Internet at http://pubs.acs.org.

References

(1) Recent reviews: (a) Ragsdale, S. W. *J. Biol. Chem.* **2009** (In press, DOI: 10.1074/jbc.R900020200). (b) Jaun, B.; Thauer, R. K. In *Metal Ions in Life Sciences*; Sigel, A., Sigel, H., Sigel, R. K. O., Eds.; John Wiley and Sons: West Sussex, U.K., 2009; Vol. 6, pp 115−132. (c) Jaun, B.; Thauer, R. K. In *Metal Ions in Life Sciences*; Sigel, A., Sigel, H., Sigel, R. K. O., Eds.; John Wiley and Sons: West Sussex, U.K., 2007; Vol. 2, pp 323−356. (d) Ragsdale, S. W. In *The Porphyrin Handbook*; Kadish, K. M., Smith, K. M., Guilard, R., Eds.; Academic Press: New York, 2003; Vol. 11, pp 205−228.

(2) Ermler, U.; Grabarse, W.; Shima, S.; Goubeaud, M.; Thauer, R. K. *Science* **1997**, *278*, 1457.

(3) (a) Pelmenschikov, V.; Blomberg, M. R. A.; Siegbahn, P. E. M.; Crabtree, R. H. *J. Am. Chem. Soc.* **2002**, *124*, 4039. (b) Pelmenschikov, V.; Siegbahn, P. E. M. *J. Biol. Inorg. Chem.* **2003**, *8*, 653.

(4) Yang, N.; Reiher, M.; Wang, M.; Harmer, J.; Duin, E. C. *J. Am. Chem. Soc.* **2007**, *129*, 11028.

(5) Dey, M.; Telser, J.; Kunz, R. C.; Lees, N. S.; Ragsdale, S. W.; Hoffman, B. M. *J. Am. Chem. Soc.* **2007**, *129*, 11030.

(6) Further computational details and related references are provided in the Supporting Information.

(7) Goenrich, M.; Mahlert, F.; Duin, E. C.; Bauer, C.; Jaun, B.; Thauer, R. K. *J. Biol. Inorg. Chem.* **2004**, *9*, 691.

(8) Hinderberger, D.; Piskorski, R. P.; Goenrich, M.; Thauer, R. K.; Schweiger, A.; Harmer, J.; Jaun, B. *Angew. Chem., Int. Ed.* **2006**, *45*, 3602.

(9) Kunz, R. C.; Horng, Y. C.; Ragsdale, S. W. *J. Biol. Chem.* **2006**, *281*, 34663.

(10) Grabarse, W.; Mahlert, F.; Duin, E. C.; Goubeaud, M.; Shima, S.; Thauer, R. K.; Lamzin, V.; Ermler, U. *J. Mol. Biol.* **2001**, *309*, 315.

(11) Wondimagegn, T.; Ghosh, A. *J. Am. Chem. Soc.* **2000**, *122*, 6375.

(12) Sarangi, R.; Dey, M.; Ragsdale, S. W. *Biochemistry* **2009**, *48*, 3146. EXAFS: extended X-ray absorption fine structure.

(13) (a) Tannor, D. J.; Marten, B.; Murphy, R.; Friesner, R. A.; Sitkoff, D.; Nicholls, A.; Ringnalda, M.; Goddard, W. A., III; Honig, B. *J. Am. Chem. Soc.* **1994**, *116*, 11875. (b) Marten, B.; Kim, K.; Cortis, C.; Friesner, R. A.; Murphy, R. B.; Ringnalda, M. N.; Sitkoff, D.; Honig, B. *J. Phys. Chem.* **1996**, *100*, 11775.

JA904301F